Mon. Not. R. Astron. Soc. **000**, 000–000 (0000) Printed 3 March 2013 (MN LATEX style file v2.2)

Halo alignments with large scale tidal and velocity fields

Sergio Contreras[1] Jaime E. Forero-Romero[1] Nelson Padilla[1]

[1] *Uni A* [2] *Uni B*

3 March 2013

ABSTRACT

Key words: methods: N-body simulations, galaxies: haloes, cosmology: theory, dark matter, large-scale structure of Universe

1 INTRODUCTION

2 THEORETICAL ANTECEDENTS

... There is abundant literature on the issue of shape and angular momentum alignment of dark matter haloe with respect to the cosmic we.

... This alignment is often measured from the distribution of the $\cos\theta$ where θ is the angle between the two axes of interest.

... Table 1 summarizes recent results found in the literature for shape and angular momentum alignment.

(Libeskind et al. 2013) (**?**) (Faltenbacher et al. 2009) (Paz et al. 2008) (Platen et al. 2008) (Lee & Erdogdu 2007)

• (Codis et al. 2012) Studies the alignment of the sping of dark matter halos realtive to the surrounding large scale structure and to the tidal tensor eigenvalues.

They use a dark matter simulation with 4096^3 DM particles in a cubic periodic box of $2000h^{-1}$Mpc on a side, which corresponds to a particle mass of $7.7 \times 10^9 \mathrm{M}_\odot$. Halos are identified using a FoF algorithm with a linking legth of 0.2 keeping all halos with more than 40 particles, which sets the minimum halo mass to be $3 \times 10^{11}\mathrm{M}_\odot$. In their work the particles were sampled on a 2048^3 grid and the density field was smoothed with a gaussian fileter over a scale of $5h^{-1}$Mpc corresponding to a mass of 1.9×10^{14}. The skeleton was computed over 6^3 overlapping subcubes and then reconnected.

The filament finder algorithm is based on Morse theory and defines a Skeleton to be the set of critical lines joining the maxima of the densit field through saddle points following the gradient. They also compute the hessinan of the potential over the smoothed density field to get their eigenvectors.

The spin of the halo is defined as $m_p \sum_i (r_i - \bar{r}) \times (v_i - \bar{v})$ where $\bar{r}$ is the center of mass of the halo and $\bar{v}$ is the average velocity.

They measure the sping alignment with each one of the eigenvectors. With repecto to the minor eigenvector e_1 there is antialignement for masses $M > 5 \times 10^{12}\mathrm{M}_\odot$and alignment for masses $< 5 \times 10^{12}\mathrm{M}_\odot$. With respect to the intermediate eigenvector e_2 there is a strong alignment at high masses and no alignment for low masses, with respecto the major eigenvector e_3 there is an anti-alignment signal at all masses. The results from the Skeleton algorithm are in perfect agreement with the results from the Tidal web. The transitional mass is weakly dependent on the smoothing scale, varing between $1 - 5 \times 10^{12}h^{-1}\mathrm{M}_\odot$for smoothing scales between $1.0 - 5.0h^{-1}$Mpc .

• (Aragón-Calvo et al. 2007) The method is the Multiscale Morphology Filter which is based on the Hessian matrix of the density field, where the density field is computed from the particle distribution using a Delaunay tesselation field estimatior (DTFE), which is self-adaptive. This allows them to identify clusters, filaments and walls.

The simulation has 512^3 particles in a cubic box of $150h^{-1}$Mpc . The mass per particle is $2 \times 10^9 h^{-1}\mathrm{M}_\odot$. Halo identitification is done with the HOP algorithm. They keep halos with more than 50 partices and less than 5000, defining a mass range of $1 - 100 \times 10^{11}h^{-1}\mathrm{M}_\odot$.

The principal axes of each halo are computed from the non-normalized inertia tensor. The inertian tensor and the angular momentum are computed with respect to the center of mass of the halo.

They compute two angles, one with respect to the direction defining the filaments and the other the walls. Their results make a distinction between halos of more massive and less massive than $10^{12}h^{-1}\mathrm{M}_\odot$.

The halo spins tend to lie on the plane of the wall. This is stronger for massive halos.The effect for filaments is weaker: low mass halos tend to lieparallel to their host filament, while high mass halos tend to be perpendicular.

Theres is a very strong effect for the principal axes of halos in filaments to be strongly correlated with the direction of the filaments. The minor axis tend to be perpendicular to the filament. This effect is stronger for larger halos.

The effect in walls is less strong ,but still the minor axis tend to lie perpendicular to the wall, while the other axis then to lie over the wall. The effect is stronger for massive halos.

They find that spins and shapes of dark matter halos are

significantly correlated with each other and with the orientation of their host structures.

• (Hahn et al. 2007)The method is the Tweb. They use three simulations each of 512^3 particles, with sizes $L_1 = 45h^{-1}$Mpc , $L_2 = 90h^{-1}$Mpc and $L_3 = 180h^{-1}$Mpc , this corresponds to particle masses of $4.7, 38.0, 300 \times 10^7 h^{-1}\mathrm{M}_\odot$. The normalization is $\sigma_8 = 0.9$. Halo identification was done with a FOF algorithm with 0.2 times the interparticle distance. They consider halos of at least 300 particles.

The web is obtained for a grid of 1024^3 cells, the density field is obtained with a CIC interpolation and smoothed using a Gaussian Kernel. In the rest of the paper all the results correspond to a smoothing scale of $R_s = 2.1h^{-1}$Mpc .

They Report on the angle between the halo angular momentum vector and the eigenvector corresponding to perpendicular directions to the sheets and the direction of the filaments. This is divided in two halo populations: $5 \times 10^{10} - 1.0 \times 10^{12}$ and $> 10^{12}$. There is a weak antialignment in the case of the filaments and a stronger antialignment in the case of the sheets. For the sheets the effect is stronger for the massive bin. In the filaments the alignment is weak regardless of the mass. They do not report any other significan statistic, but recognize that they suffer from small-number statistics in voids).

They do not see any strong dependance of the environment in the shape. They do not measure the shape alinment.

• (Basilakos et al. 2006) Use a cosmological SPH+N-body simulation to measure the alignment of cluster halos with their parent supercluster. For both the cluster halos and parent super-cluster they define the shape via the non-normalized inertia tensor. The find that strenght of the alignments increases with the degree of filamentarity of the supercluster.

The simulation has 2×512^3 particles in a box of side $500h^{-1}$Mpc . The dark matter particle mass is $6.6 \times 10^{10} h^{-1}\mathrm{M}_\odot$while for SPH particles is $1.2 \times 10^{10} h^{-1}\mathrm{M}_\odot$. The halo finding is done with a FOF algorithm with a linking length of 0.17 and keep objects with more than 100 partcles.

• (Lee & Pen 2002)Observational measurement for the alignment of galaxy spin axes with the local tidal shear field. For the measurement of shear, we have used the Point Source Catalog Redshift (PSCz) survey (a complete redshift survey from the IRAS Point Source Catalog) data. This was done down to a radial comoving distance of $\sim 150h^{-1}$Mpc .

• (Hatton & Ninin 2001) DM matter only simulation. 256^3 particles, $100h^{-1}$Mpc , particle mass. Look for mutual alignment of angular momentum vectors, and alignment with structure. halos on any escale by close pair statistics. They don't find any evidence for a statistically significant mutual alignment of haloes on any scale,

3 N-BODY SIMULATION AND HALO FINDING

... In this paper we use groups found with a FOF halo finder.

4 THE COSMIC WEB ALGORITHMS

4.1 The Tidal Web

4.2 The Velocity Web

4.3 Numerical considerations

... In this paper we compute the cosmic web on grids of two different resolutions 256^3 and 512^3.

5 RESULTS

5.1 Interweb Alignment

... We compute the pair-wise allignment between the eigenvectors in the two web finders.

... We also compute the alignment between the eigenvectors in cells occupied by dark matter halos. This will be a key element in the interpretation of the results for halo-based allignments in the next sections: shape, angular momentum and peculiar velocities.

...

5.2 Shape Alignment

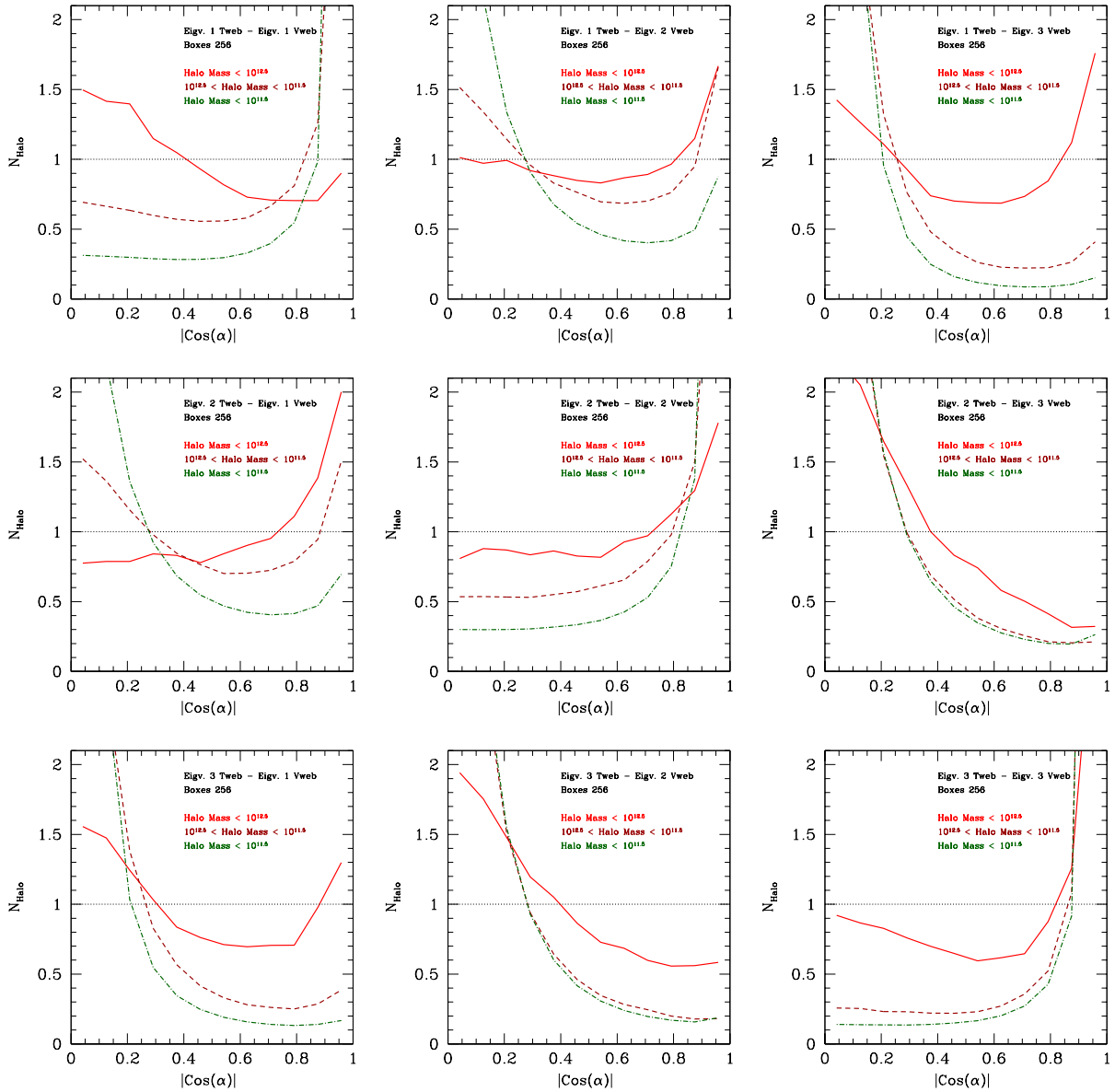

Figure 1. Interweb alignment for 256^3 grid resolution.

5.3 Angular Momentum Alignment

5.4 Peculiar velocity Alignment

6 DISCUSSION

7 CONCLUSIONS

ACKNOWLEDGMENTS

REFERENCES

Aragón-Calvo M. A., van de Weygaert R., Jones B. J. T., van der Hulst J. M., 2007, ApJL, 655, L5

Basilakos S., Plionis M., Yepes G., Gottlöber S., Turchaninov V., 2006, MNRAS, 365, 539

Codis S., Pichon C., Devriendt J., Slyz A., Pogosyan D., Dubois Y., Sousbie T., 2012, MNRAS, 427, 3320

Faltenbacher A., Li C., White S. D. M., Jing Y.-P., Shu-DeMao Wang J., 2009, Research in Astronomy and Astrophysics, 9, 41

Hahn O., Carollo C. M., Porciani C., Dekel A., 2007, MNRAS, 381, 41

Hatton S., Ninin S., 2001, MNRAS, 322, 576

Lee J., Erdogdu P., 2007, ApJ, 671, 1248

Lee J., Pen U.-L., 2002, ApJL, 567, L111

Libeskind N. I., Hoffman Y., Forero-Romero J., Gottlöber S., Knebe A., Steinmetz M., Klypin A., 2013, MNRAS, 428, 2489

Paz D. J., Stasyszyn F., Padilla N. D., 2008, MNRAS, 389, 1127

Platen E., van de Weygaert R., Jones B. J. T., 2008, MNRAS, 387, 128

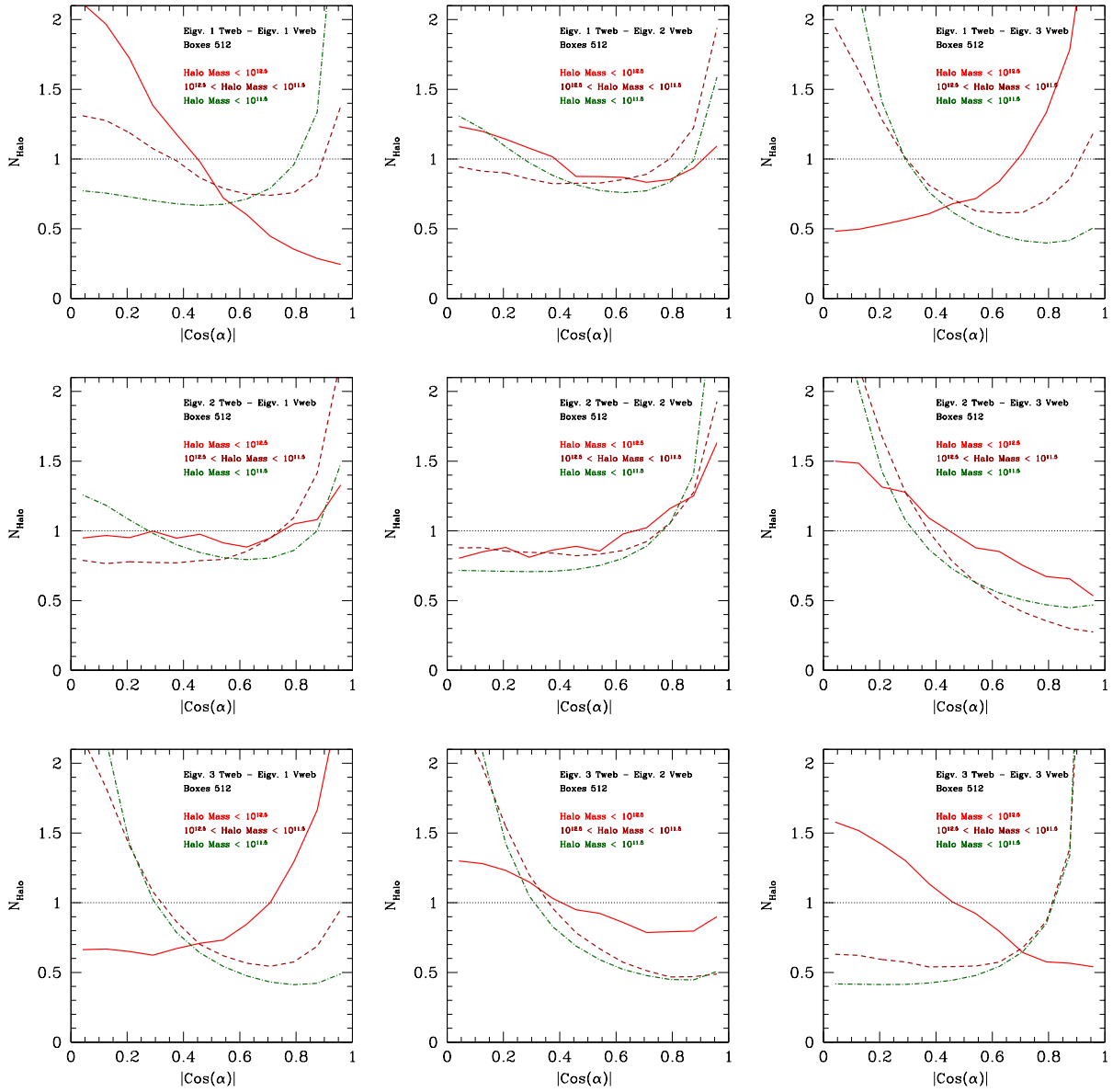

Figure 2. Interweb alignment for 512^3 grid resolution.

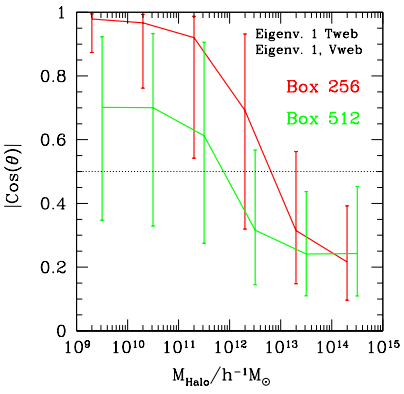

Figure 3. Median of the interweb alignment for the two grid resolution.

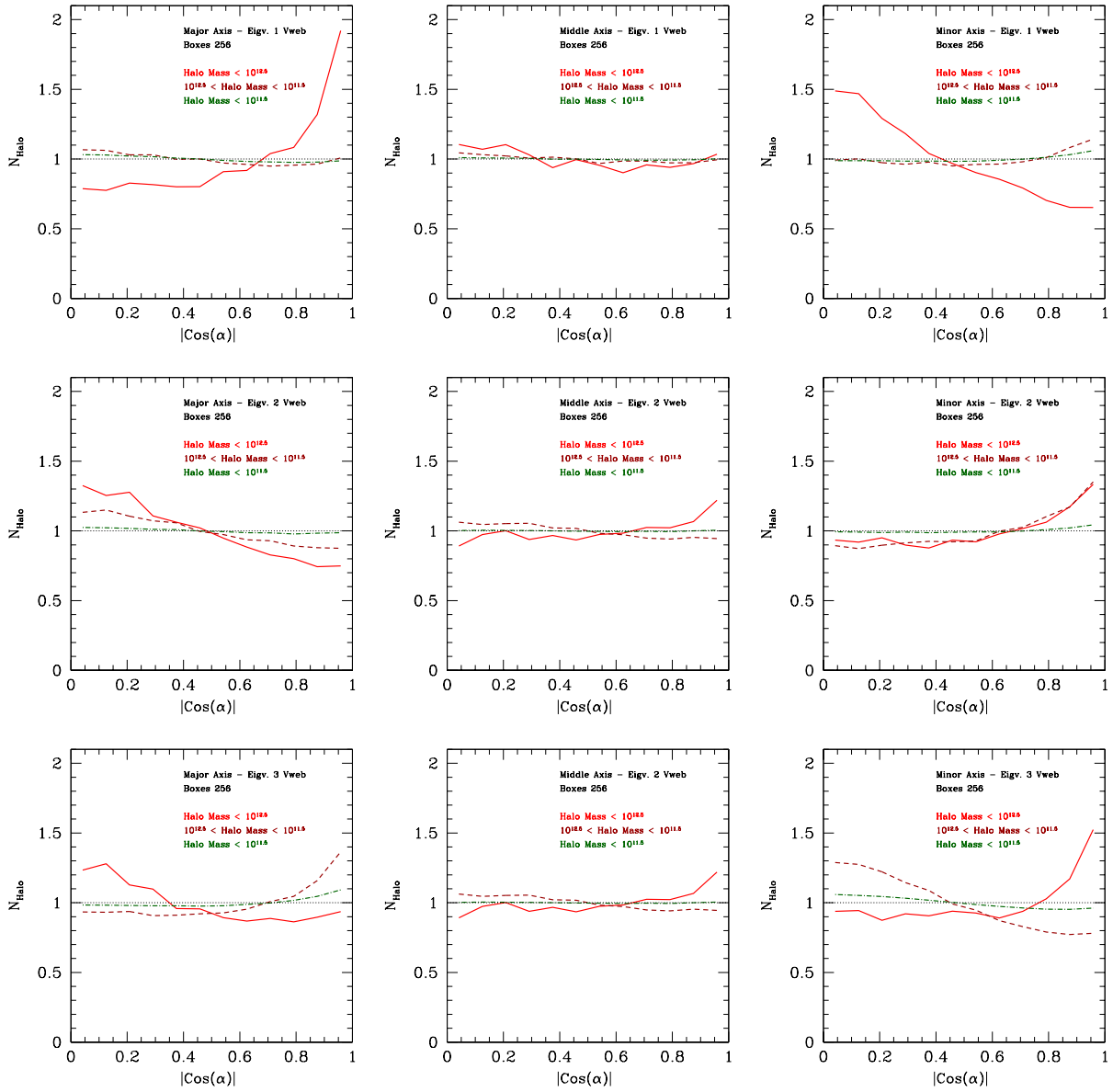

Figure 4. Shape alignment for the vweb at 256^3 resolution.

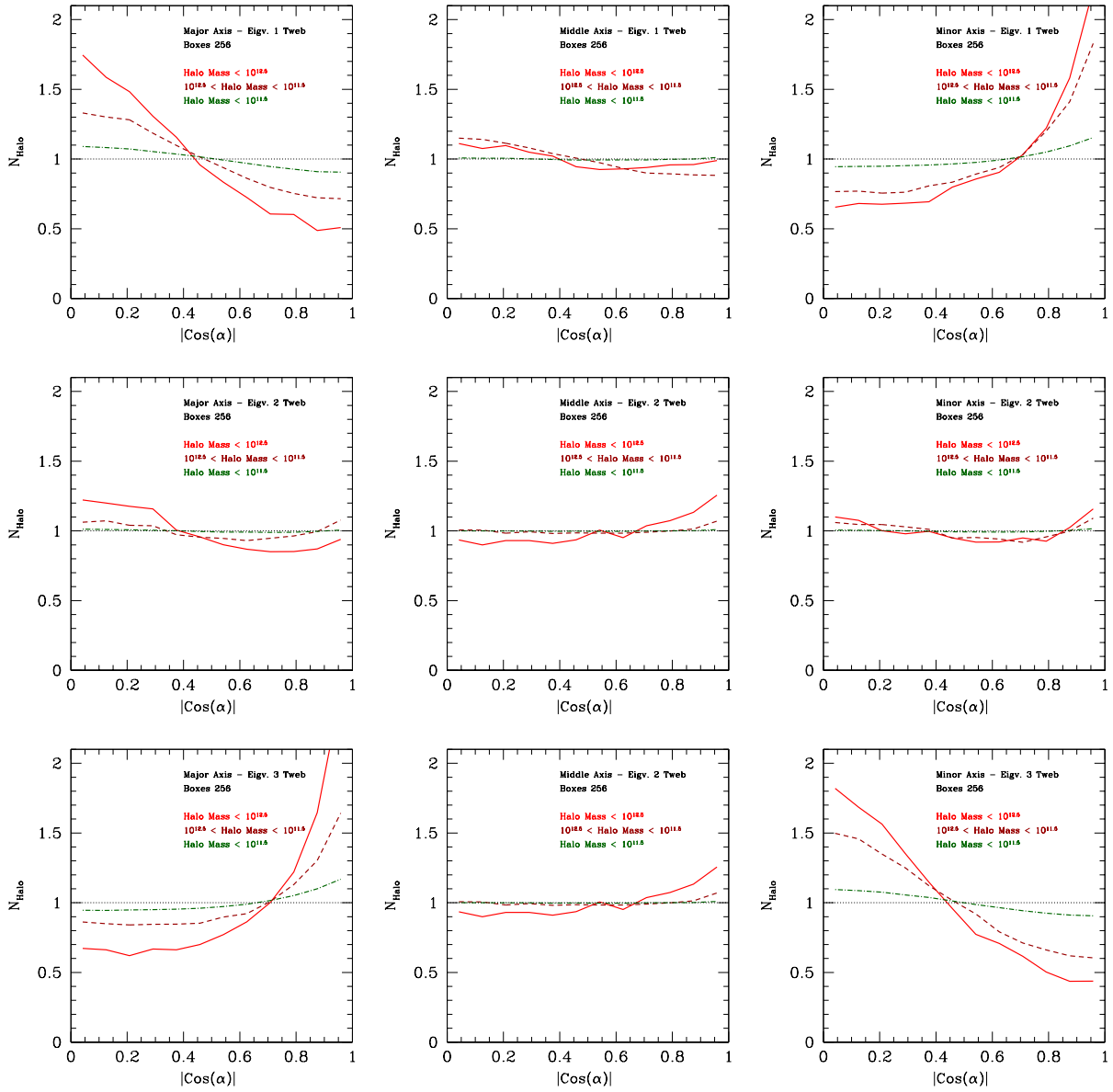

Figure 5. Shape alignment for the tweb at 256^3 resolution.

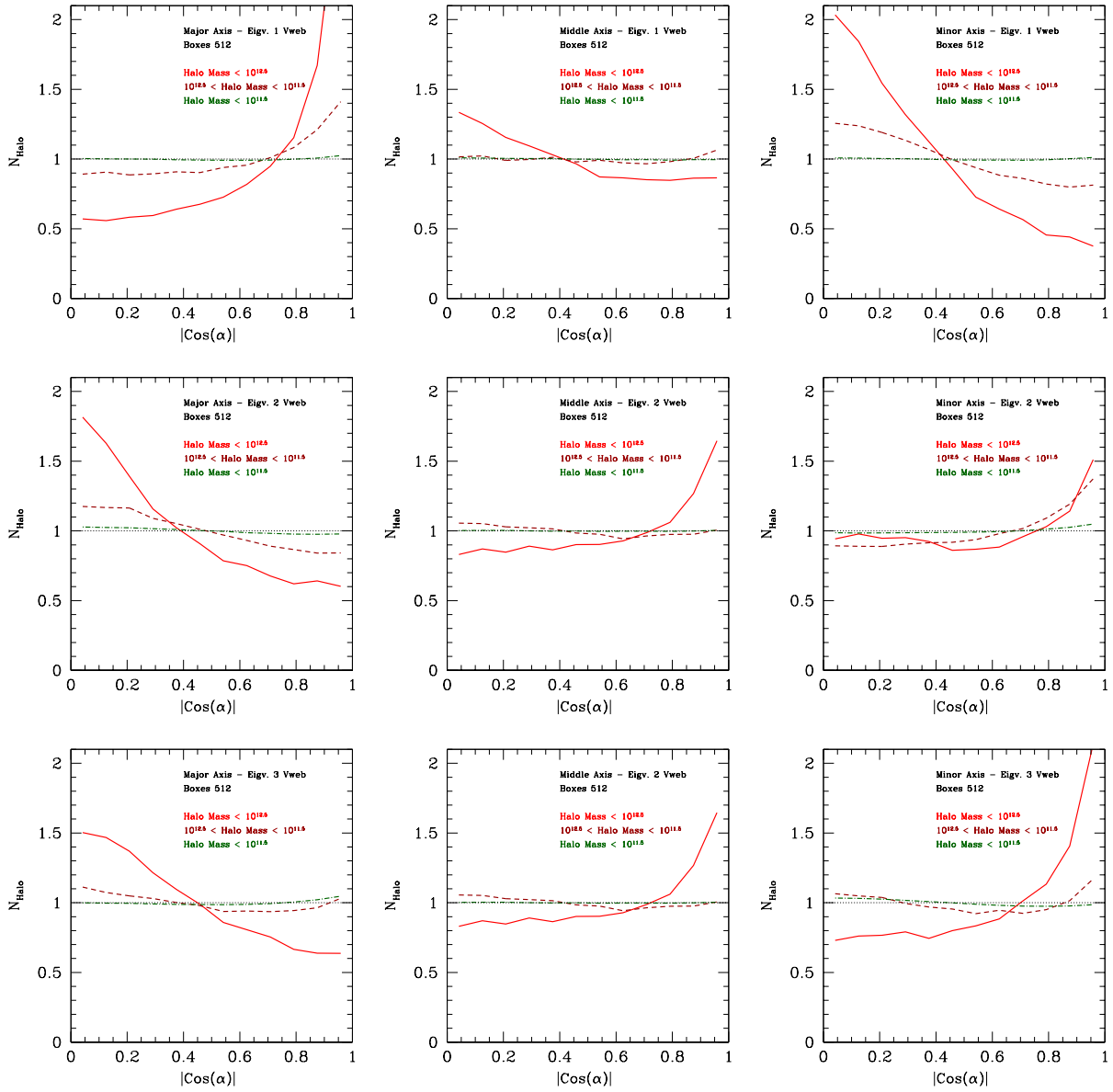

Figure 6. Shape alignment for the vweb at 512^3 resolution.

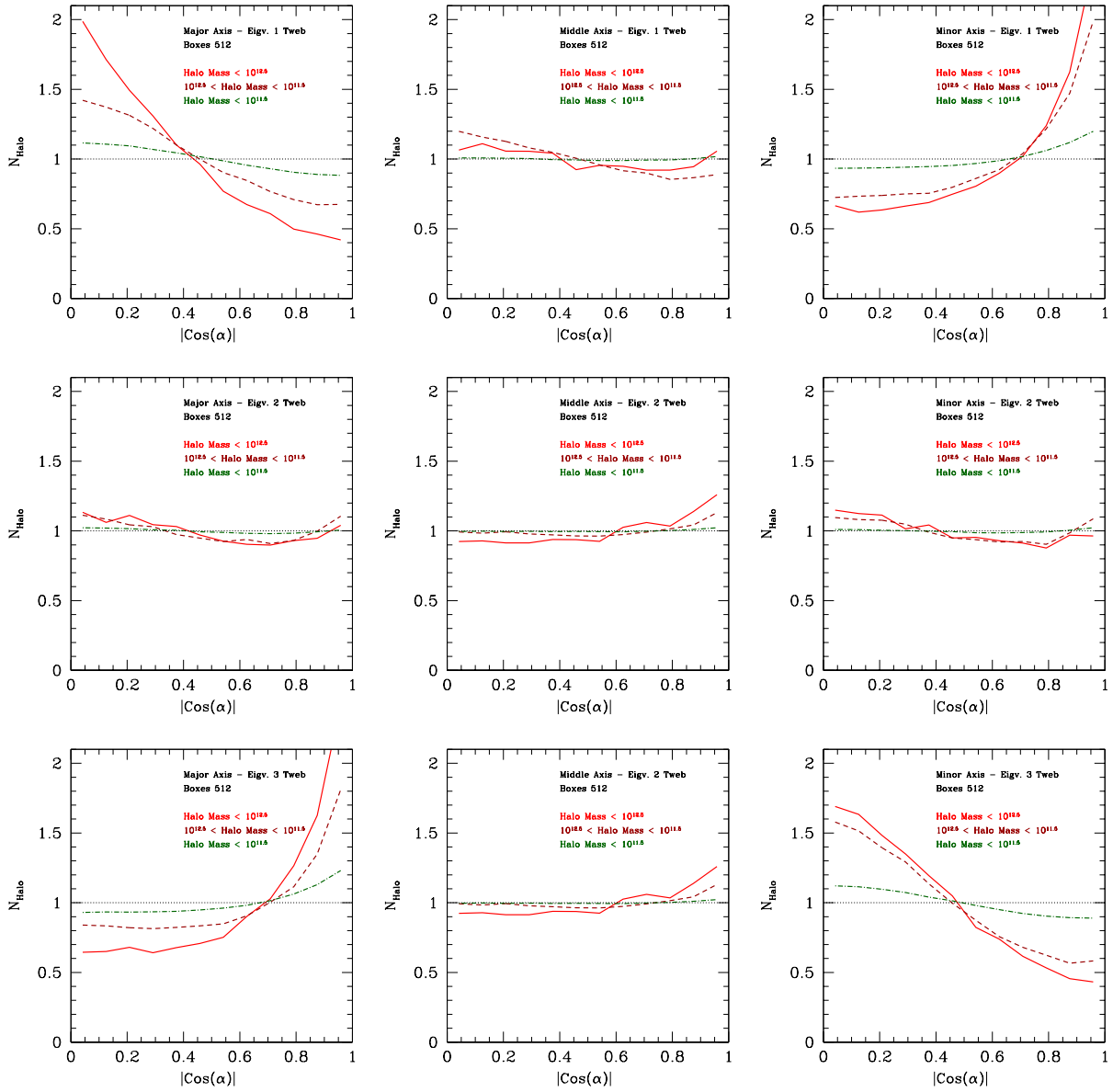

Figure 7. Shape alignment for the tweb at 512^3 resolution.

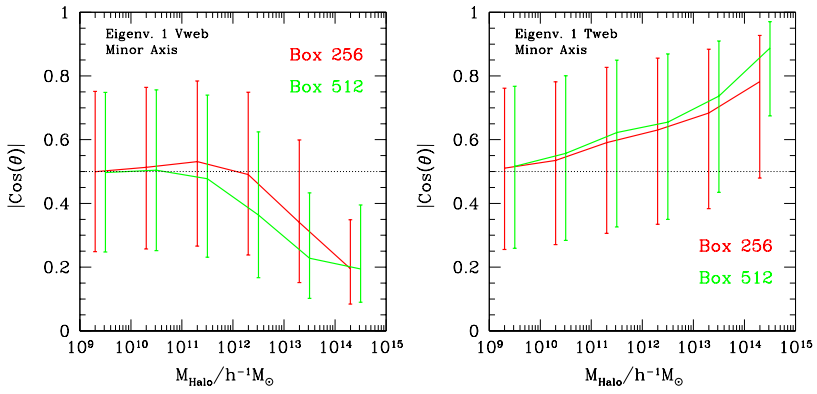

Figure 8. Median of the shape alignment for the two web and the two grid resolution.

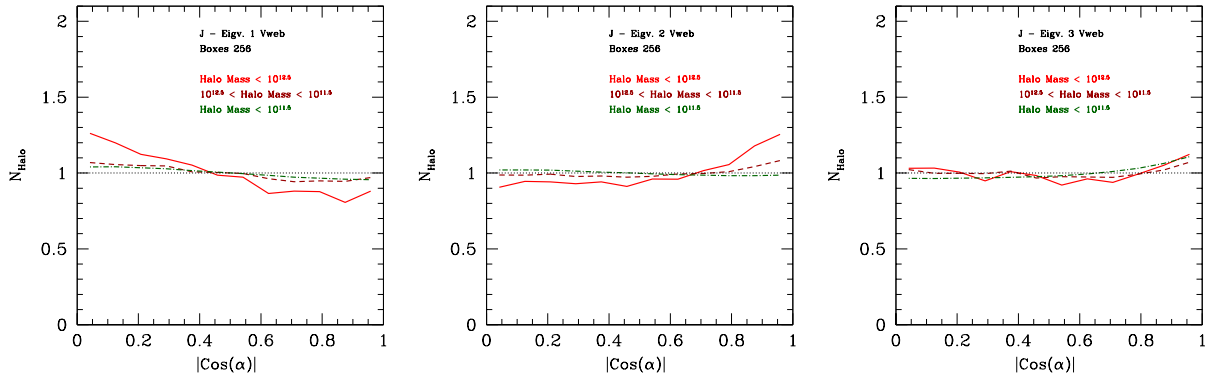

Figure 9. Angular momentum alignment with the Vweb for 256^3 grid resolution.

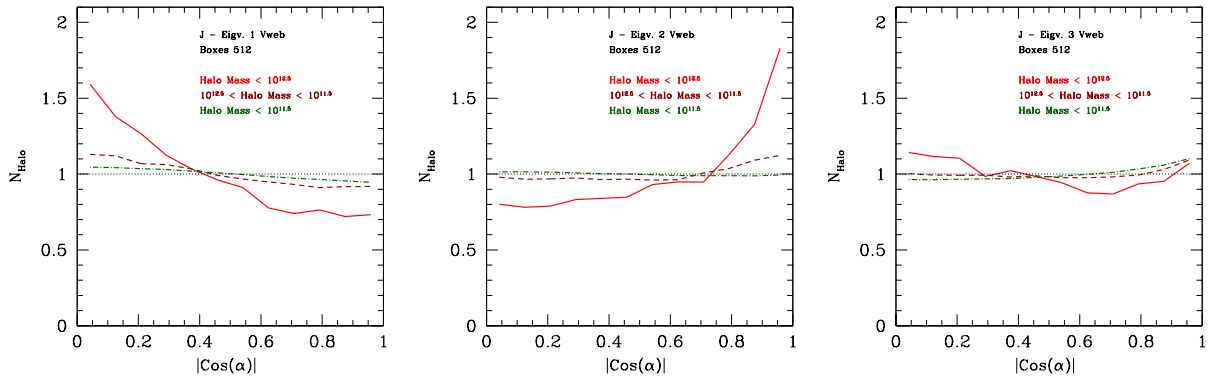

Figure 10. Angular momentum alignment with the Vweb for 512^3 grid resolution.

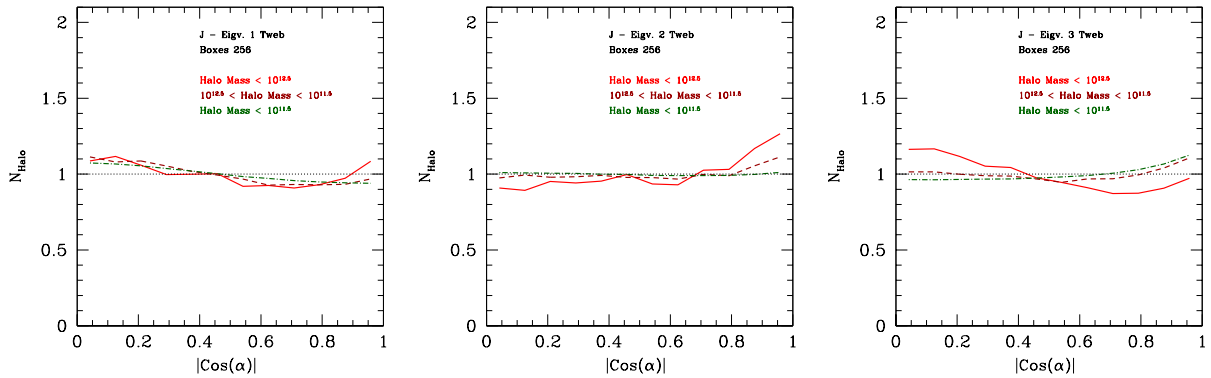

Figure 11. Angular momentum alignment with the Tweb for 256^3 grid resolution.

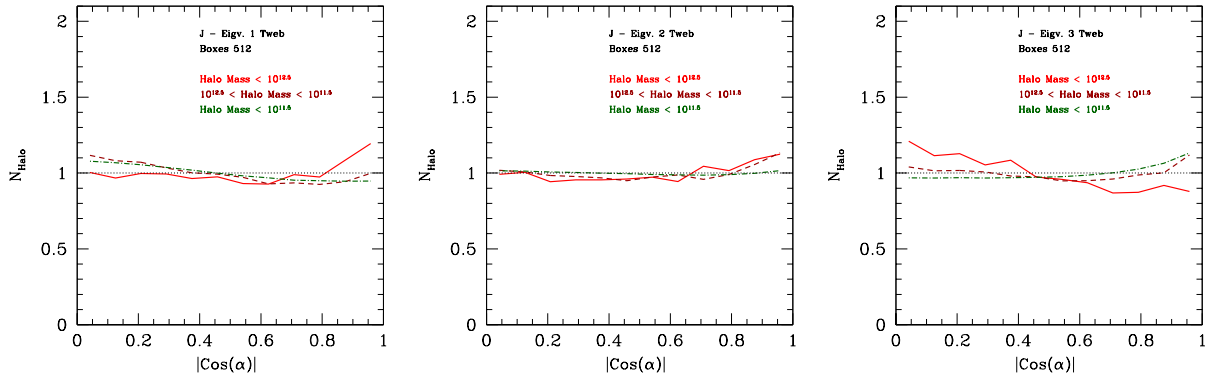

Figure 12. Angular momentum alignment with the Tweb for 512^3 grid resolution.

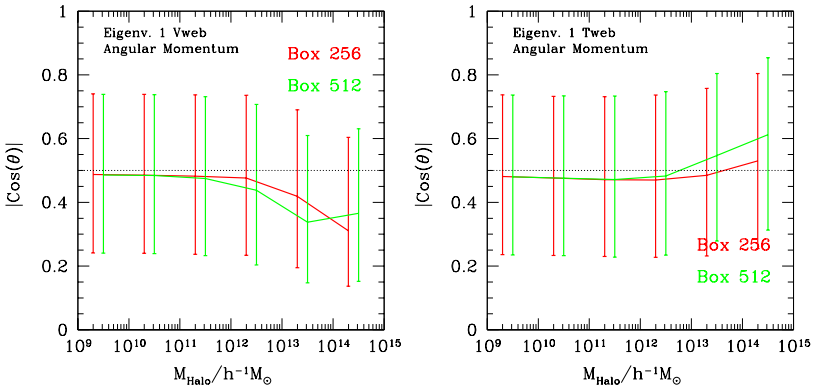

Figure 13. Median of the angular momentum for the two web and the two grid resolution.

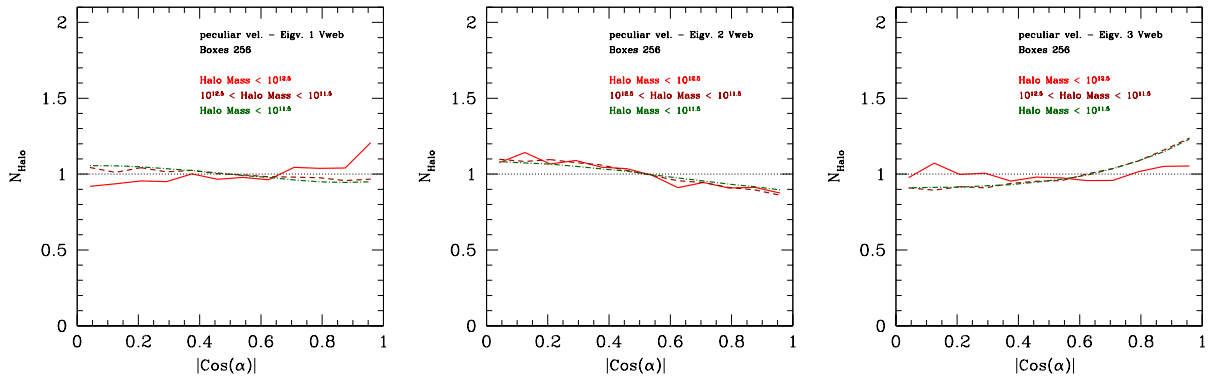

Figure 14. Peculiar velocity alignment with the Vweb for 256^3 grid resolution.

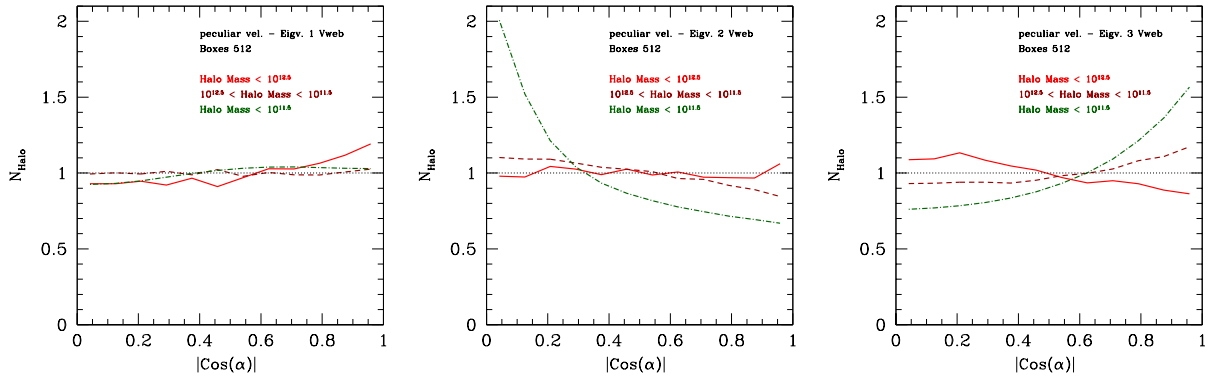

Figure 15. Peculiar velocity alignment with the Vweb for 512^3 grid resolution.

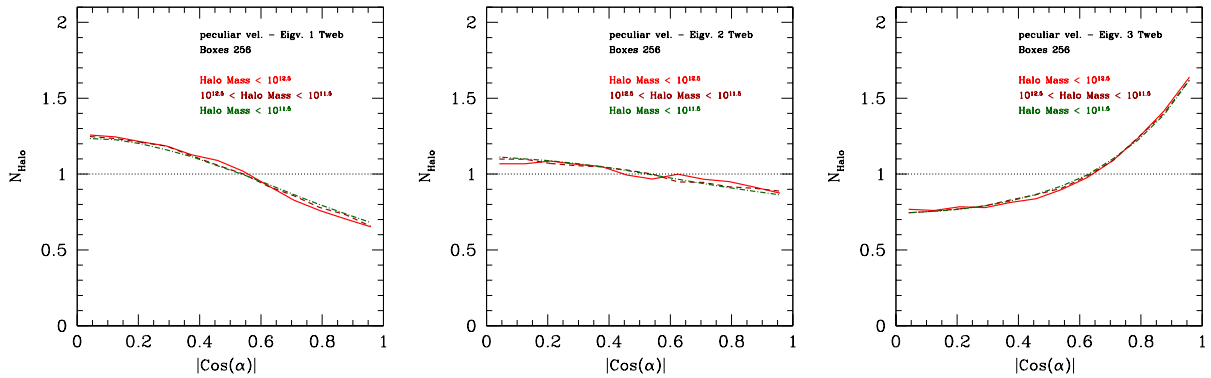

Figure 16. Peculiar velocity alignment with the Tweb for 256^3 grid resolution.

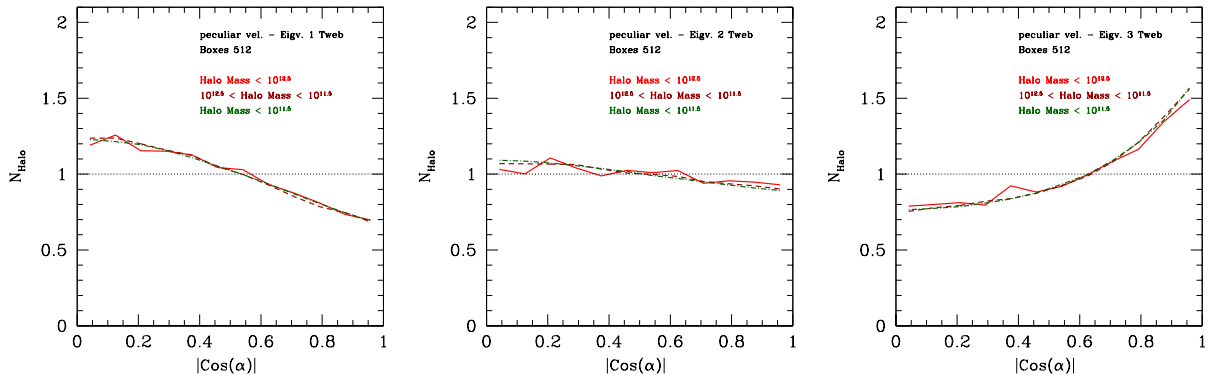

Figure 17. Peculiar velocity alignment with the Tweb for 512^3 grid resolution.

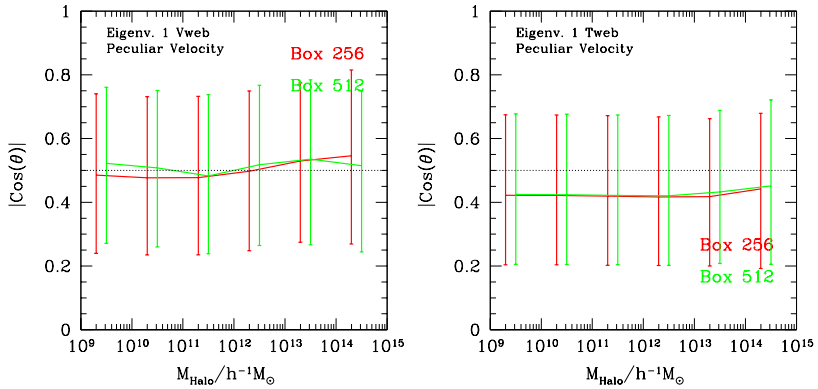

Figure 18. Median of the peculiar velocity for the two web and the two grid resolution.